Chemical Science

ROYAL SOCIETY OF CHEMISTRY

EDGE ARTICLE

View Article Online
View Journal





Cite this: DOI: 10.1039/d5sc10082h

All publication charges for this article have been paid for by the Royal Society of Chemistry

Received 23rd December 2025
Accepted 15th April 2026

DOI: 10.1039/d5sc10082h

rsc.li/chemical-science

# *Ortho*-Methylation of pyridine *via* intramolecular *N*-methyl migration

Shun-Yao Huang,†[a] Shun Li,†[b] Ming-Yuan Li,[a] Cong Lv,[a] Shen-Xiang Wang,[a] Wei-Chao Xue,[a] Jia-Qi Xu,[a] Xue-Li Zheng,[a] Rui-Xiang Li,[a] Hua Chen*[a] and Hai-Yan Fu*[a]

Pyridine is a privileged scaffold in pharmaceuticals, and selective C2-alkylation, particularly methylation, represents a valuable strategy to fine-tune drug-like properties such as metabolic stability and solubility. However, achieving highly site-selective methylation at the C2 position remains challenging. Herein, we report a ruthenium-catalyzed, copper-mediated protocol that enables direct C2-methylation of pyridines. The transformation proceeds through a formal *N*-to-C methyl migration in *N*-methylpyridinium salts, which serve dually as activated substrates and internal methyl donors, thereby ensuring excellent atom economy. This operationally simple and scalable approach is compatible with the late-stage modification of complex bioactive molecules. Furthermore, the migratable groups can be extended to longer alkyl and benzyl substituents, highlighting the broad synthetic utility of this strategy.

## Introduction

The methyl group, despite being the simplest alkyl unit, exhibits a remarkable ability to modulate biological activity and physicochemical properties—a phenomenon widely recognized in medicinal chemistry as the "magic methyl effect". Notable examples include a 208-fold potency increase in a p38α MAP kinase inhibitor and a 2135-fold enhancement for the S1P1 antagonist NIBR-0213 upon a single C–H methylation. [1] Pyridine is a privileged scaffold commonly found in pharmaceuticals, many of which contain methyl-substituted variants—particularly at the 2-position—as exemplified by several drugs (Scheme 1A).[2] In this context, the development of methods for the C2-selective methylation of pyridine is of great importance in medicinal chemistry.[3]

However, the landscape of regioselective pyridine methylation reveals distinctly different challenges across positions.[4] Notably, significant advances have been made in recent years to address these selectivity issues. For the inherently low-reactivity *meta*-position,[5] elegant dearomatization-methylation-rearomatization sequences have emerged as robust solutions, exemplified by contributions from Donohoe,[3e] Wang,[6] and others.[7] In contrast, achieving selective methylation at the C2 and C4 positions is complicated by their electronic similarity and competing reactivity.[8,9] Sporadic examples using nucleophilic reagents such as Wittig reagents[3d] and diborylmethane[10] have been reported, but general and reliable regiocontrol remains limited. This issue is particularly pronounced in Minisci-type radical methylation.[11] Despite elegant demonstrations by MacMillan,[3a] Li[3b] and others[3c] employing methanol as a methyl source under photochemical conditions, competing C4 addition persists, compromising the selectivity (Scheme 1B). Therefore, achieving exclusive C2-methylation within a radical framework continues to represent an unmet and notable challenge.

Recently, *N*-functionalized pyridinium salts have emerged as versatile radical precursors. Their low reduction potentials enable them to act as competent single electron acceptors. Upon reduction, the resultant pyridiniumyl radical cations fragment, liberating radical species for diverse transformations.[12] This paradigm is well-established with precursors like *N*-alkoxypyridinium salts and *N*-amidopyridinium salts, as demonstrated in the elegant studies of Stephenson,[13] Sungwoo Hong,[14] and others.[15] These precursors typically generate O- or N-centered radicals, which subsequently undergo β-scission or radical rearrangement to deliver C-centered radicals that participate in pyridine alkylation.[16] In parallel, Katritzky salts (*N*-alkylpyridinium salts derived from the 2,4,6-triphenylpyrylium compound) have become widely used as practical alkyl radical precursors.[17] However, this approach intrinsically consumes the triphenylpyridine scaffold, leading to poor atom economy and limited substrate scope (Scheme 1C).[18] Methyl iodide readily undergoes *N*-methylation with pyridine to afford *N*-methylpyridinium salts, which represent the simplest members of this family. However, the generation of methyl radicals from *N*-methylpyridinium salts for the

[a]*Key Laboratory of Green Chemistry & Technology, Ministry of Education, College of Chemistry, Sichuan University, Chengdu, Sichuan 610064, China. E-mail: scufhy@scu.edu.cn*

[b]*College of New Energy Materials and Chemistry, Leshan Normal University, Leshan, Sichuan 614000, China*

† These authors contributed equally to this work.

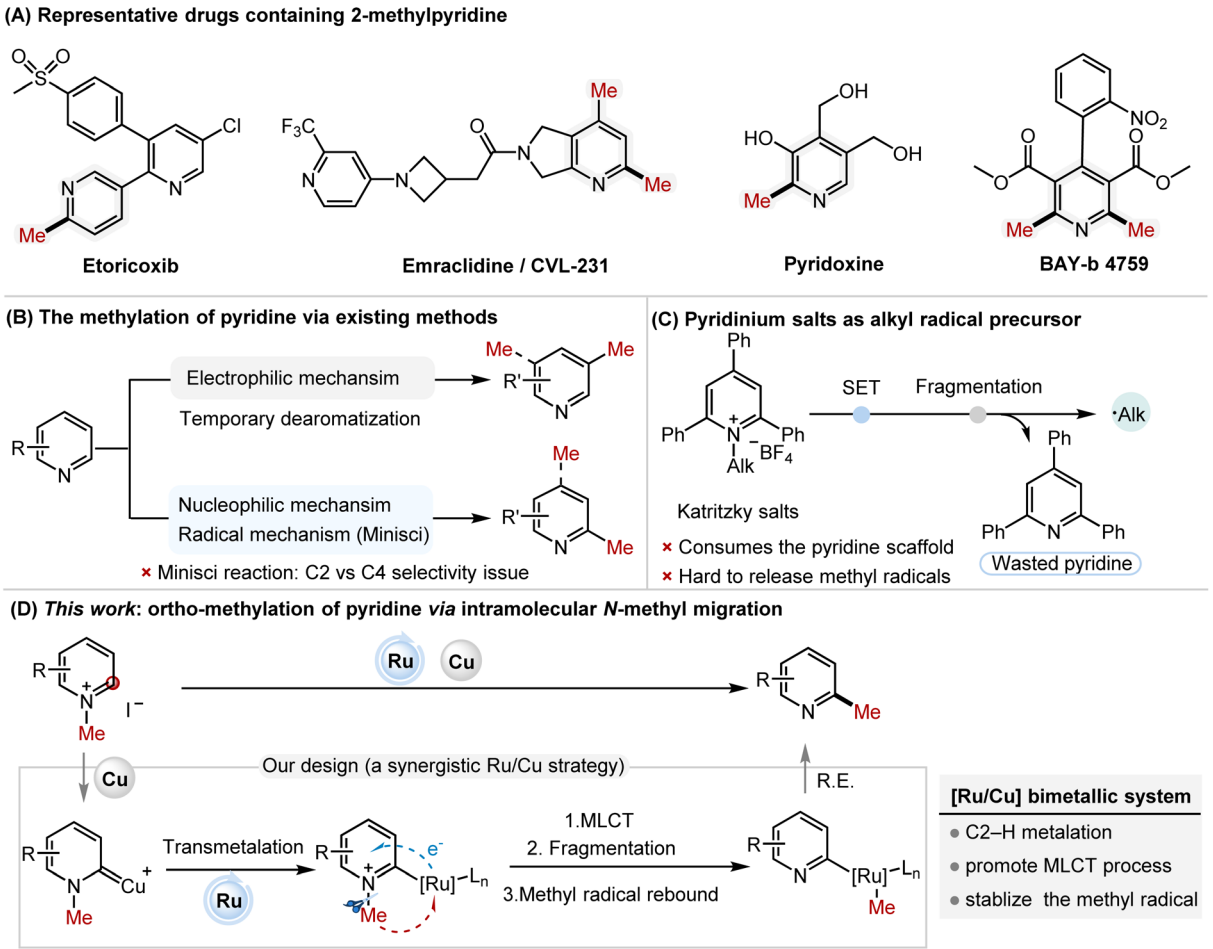


Scheme 1 Strategies for the methylation of pyridines: (A) representative drugs containing 2-methylpyridine, (B) the methylation of pyridine *via* existing methods, (C) pyridinium salts as radical precursors, (D) this work: *ortho*-methylation of pyridine *via* intramolecular *N*-methyl migration.

methylation reaction has not yet been achieved, probably because the highly reactive and short-lived methyl radical is difficult to control.[11b,19]

Herein, we designed a Ru/Cu bimetallic system that utilizes an *N*-methylpyridinium salt as both the methyl radical source and the activated substrate, enabling the site-selective C2-methylation of pyridine. A Cu(I) salt was employed to promote regioselective C2–H metalation of the pyridinium ring, leveraging the intrinsic preference of Cu(I) for coordination at the C2 position of pyridinium salts.[20] The resulting C2–Cu intermediate is proposed to undergo transmetalation with a ruthenium species, generating a pyridyl–Ru complex. Considering the well-established metal-to-ligand charge transfer (MLCT) characteristics of Ru(II)–polypyridyl complexes,[21] we proposed that a pyridiniumyl-Ru species could undergo intramolecular single-electron transfer (SET) from the Ru(II) center to the electronically more deficient pyridiniumyl ligand. This SET process would generate an *N*-methylpyridinium radical intermediate that subsequently fragments *via* N–C bond cleavage to release a methyl radical.[12b] The reactive methyl radical is stabilized by rapid rebound with the pyridyl-ligated ruthenium center. Finally, reductive elimination from the Ru center would deliver the desired C2-methylated pyridine. These sequences finally accomplish a formal *N*-to-C2 methyl migration, thereby providing a viable solution to the long-standing challenge of achieving exclusive C2-methylation of pyridines.

Table 1 Optimization of reaction conditions[a]

| Entry | Deviation from standard conditions | 1 (%)[b] |
|---|---|---|
| 1 | None | 87 (78)[c] |
| 2 | w/o $Ru(COD)Cl_2$ | n.d. |
| 3 | 5 mol% of $Ru(COD)Cl_2$ | 63 |
| 4 | w/o CuI | n.d. |
| 5 | 2 equiv.CuI | 47 |
| 6 | 1 equiv. CuI | 16 |
| 7 | w/o PivOK | Trace |
| 8 | w/o PivOH | 53 |
| 9 | Diglyme as the solvent | 45 |
| 10 | Under air | 46 |
| 11 | $T = 120$ °C | 53 |

[a] Unless otherwise noted, all of the reactions were carried out with **1a** (0.25 mmol), $Ru(COD)Cl_2$ (10 mol%), CuI (3.0 equiv.), PivOK (2.0 equiv.), PivOH (1.0 equiv.), diglyme/monoglyme (v : v 9 : 1, 1.0 mL), $N_2$, 140 °C, and 16 h. [b] Isolated yields. [c] value in parentheses denotes gram-scale reaction (5 mmol).

## Results and discussion

To verify the feasibility of this mechanistic design, we selected *N*-methyl-2-phenylpyridinium iodide (**1a**) as the model substrate for investigation under a ruthenium/copper bimetallic system. Pleasingly, the initial experiments confirmed the formation of the desired 1,2-methyl migration product (**1**), validating our proposed approach. Subsequent systematic optimization of the reaction parameters (SI Tables S1–S8) established the optimal conditions as follows: $Ru(COD)Cl_2$ (10 mol%) as the catalyst, CuI (3.0 equiv.) as the Cu(I) source, PivOK (2.0 equiv.) as the base, and PivOH (1.0 equiv.) as the acidic additive in a 9 : 1 diglyme/monoglyme solvent mixture, heated at 140 °C for 16 h in a sealed tube under an $N_2$ atmosphere. Under these conditions, product **1** was isolated in 87% yield, and the transformation was readily scalable to the gram scale without appreciable loss in efficiency (Table 1, entry 1). Control experiments underscored the critical roles of both $Ru(COD)Cl_2$ and CuI. Omission of $Ru(COD)Cl_2$ completely suppressed product formation, and lowering its loading substantially decreased the yield (entries 2 and 3). Similarly, CuI was also essential; no desired product was detected in its absence, and each 1.0 equiv. reduction in its loading resulted in an approximate 30% decrease in yield (entries 4, 5 and 6). Among the bases

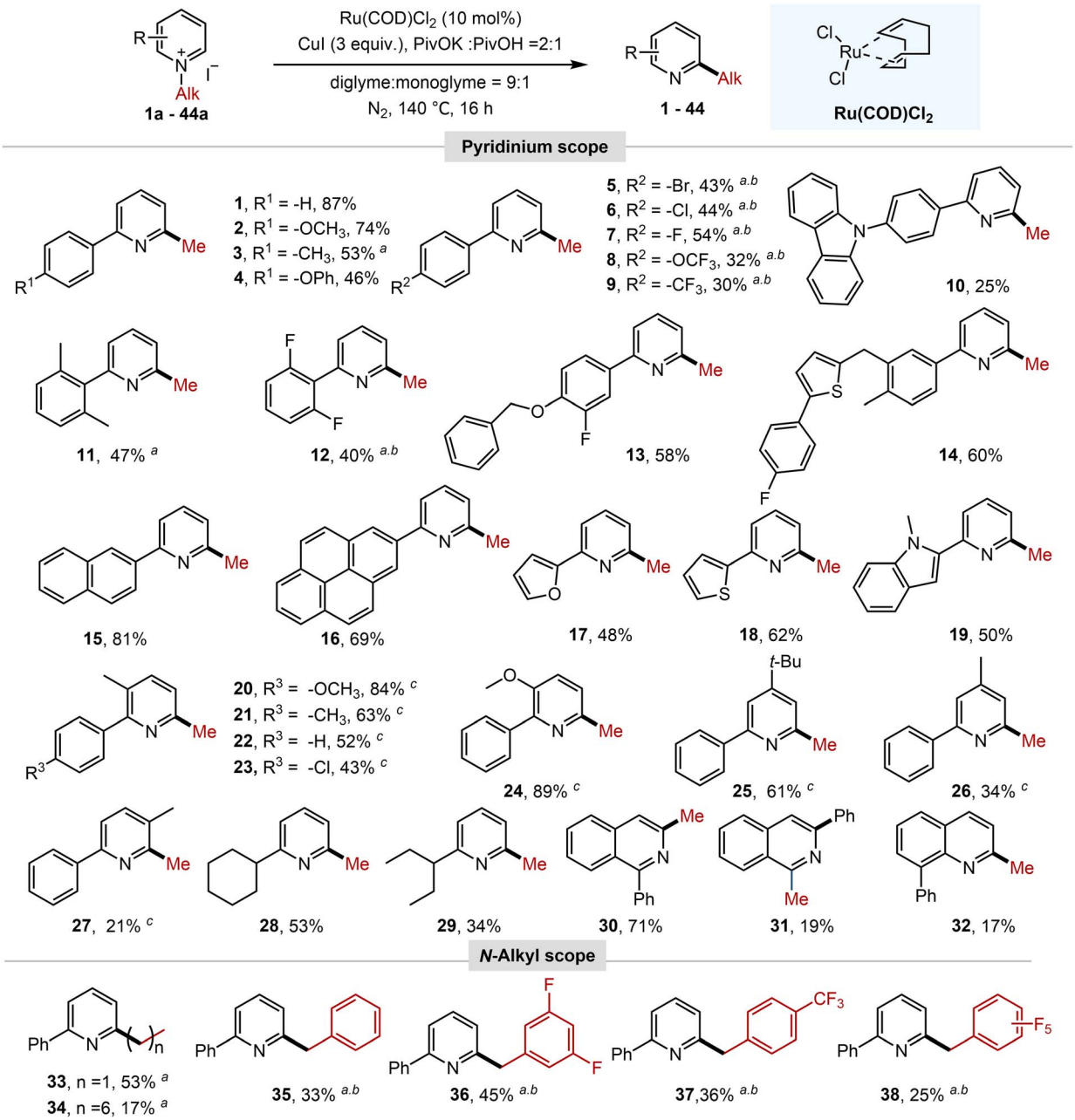


Scheme 2 The scope of substrates. Reaction conditions: *N*-alkylpyridinium salt (0.25 mmol), $Ru(COD)Cl_2$ (10 mol%), CuI (3.0 equiv.), PivOK (2.0 equiv.), PivOH (1.0 equiv.), diglyme/monoglyme (v : v 9 : 1, 1.0 mL), $N_2$, 140 °C, and 16 h. Isolated yields. [a]24 h. [b]CuBr instead of CuI. [c]36 h.

screened, PivOK was uniquely effective; in its absence, only trace amounts of the desired product were detected (entry 7). Intriguingly, its conjugate acid PivOH was also beneficial—its removal caused a pronounced drop in yield (entry 8). The solvent composition was found to be critical, with the 9 : 1 diglyme/monoglyme solvent mixture proving optimal; the use of neat diglyme significantly compromised the yield (entry 9). A nitrogen atmosphere was essential to prevent Cu(I) intermediate oxidation at elevated temperature (entry 10). Finally, reducing the reaction temperature to 120 °C led to a markedly lower yield (entry 11).

With optimized conditions established, the substrate scope was systematically evaluated for *N*-methyl-2-arylpyridinium salts, as summarized in Schemes 2 and 3. Initial studies focused on electronic effects at the aryl ring. *para*-Electron-donating groups (–$OCH_3$, –$CH_3$, and –OPh) afforded moderate yields (46–74%, **2–4**). In contrast, *para*-electron-withdrawing substituents (–Br, –Cl, –F, –$OCF_3$, and –$CF_3$) markedly suppressed the reaction. However, by replacing CuI with CuBr and extending the reaction time, the corresponding product was obtained in moderate yields (30–54%, **5–9**). Furthermore, the reaction scope could be extended to a 2-arylpyridinium salt bearing a *para*-carbazolyl group, which delivered the corresponding product **10** in a synthetically useful yield. Remarkably, the 2-aryl group of the pyridinium salts tolerated disubstitution patterns from 3,4-disubstituted to sterically hindered 2,6-disubstituted variants, as well as diverse functional groups (*e.g.*, alkyl, ether, heterocycles, halogens, *etc.*), allowing efficient conversion to the desired products (**11–14**). Methyl migration proceeded with high efficiency for *N*-methylpyridinium salts bearing extended π-conjugated systems, such as 2-naphthyl and 2-pyrenyl substituents, affording products **15** and **16** in 81% and 69% yield, respectively. The reaction was also compatible with C2-heteroaryl substrates, which underwent methyl migration to deliver products in moderate yields (**17–19**). It should be noted that pyridinium rings bearing substituents at C3, C4, or C5 positions remained competent substrates, though efficiency varied with substitution patterns (**20–27**).

Crucially, the C2-aryl group proved indispensable; *N*-methylpyridinium salts lacking this moiety exhibited complete suppression of methyl migration (SI Fig. S6). This is likely because the C2-aryl group stabilizes the radical species generated upon SET from Ru(II) to the pyridinium moiety.[12b,19a] For 2-alkyl-substituted *N*-methylpyridinium salts, the reactivity is highly dependent on the alkyl chain structure. α-Branched alkyl groups, for example, cyclohexyl and pentan-3-yl, afforded products in synthetically useful to moderate yields (**28**, **29**), while linear alkyl chains yielded only trace amounts of products under standard conditions (SI Fig. S6), likely due to deprotonation of the benzylic C–H bond under basic conditions to form alkylidene-1-methyl-1,2-dihydropyridines, thereby inhibiting the desired reaction. The protocol could be extended to *N*-methylquinolinium and *N*-methylisoquinolinium salts bearing an *ortho*-aryl group, as exemplified by compounds **30–32**. In addition to *N*-methylpyridinium salts, other types of *N*-alkyl groups on pyridinium salts could also migrate to generate corresponding products. For those bearing straight-chain *N*-alkyl substituents, reaction efficiency inversely correlated with chain length, yielding products **33–34** with diminished efficiency. In the *N*-benzyl series, moderate electron-withdrawing substituents were generally beneficial (**35–37**), whereas the strongly electron-deficient perfluorobenzyl group resulted in significantly reduced yield (**38**).

The developed Ru/Cu synergistic strategy enables efficient late-stage modification of pyridine-containing drugs and their analogues. For example, Loratadine, a pyridine-based anti-

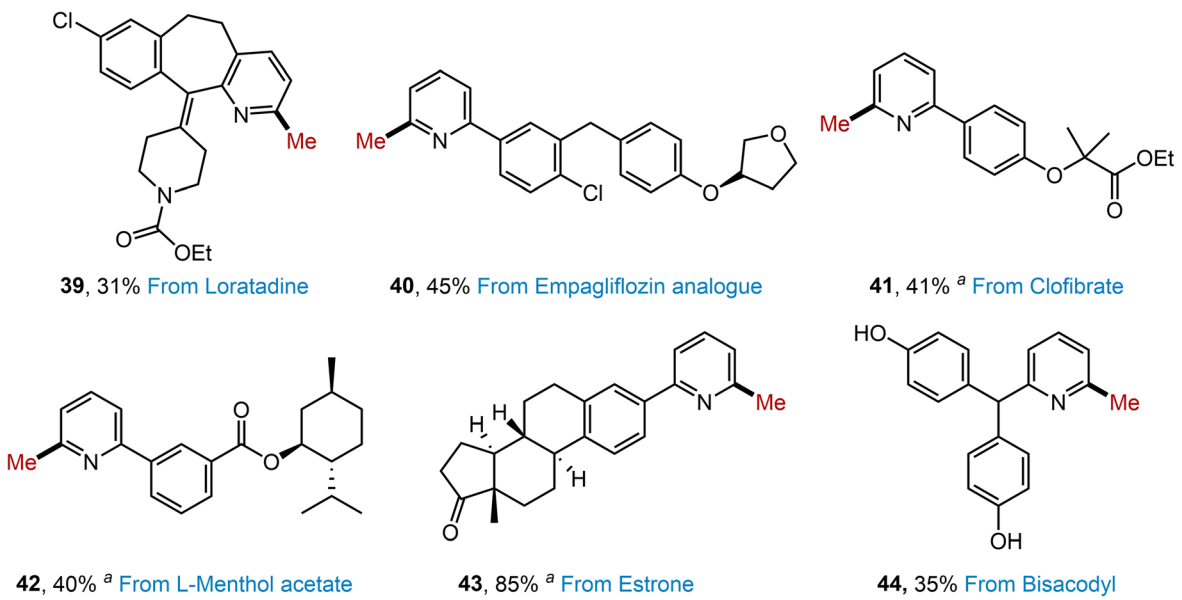


Scheme 3 Late-stage methylation of pyridine-containing drugs and drug-like compounds. Reaction conditions: *N*-alkylpyridinium salt (0.25 mmol), $Ru(COD)Cl_2$ (10 mol%), CuI (3.0 equiv.), PivOK (2.0 equiv.), PivOH (1.0 equiv.), diglyme/monoglyme (v : v 9 : 1, 1.0 mL), $N_2$, 140 °C, and 16 h. Isolated yields. [a]CuBr instead of CuI.

allergy drug, was successfully transformed into its C2-methylated analogue (**39**). Substrates derived from the empagliflozin analogue (**40**), clofibrate (**41**), L-menthol acetate (**42**) and estrone (**43**) were also viable substrates for this strategy, affording corresponding *ortho*-methylated derivatives. Bisacodyl, a stimulant laxative containing an acetoxy group, underwent a methyl migration accompanied by acetoxy hydrolysis, yielding the C2-methylated product **44** in 35% yield.

To gain insight into the reaction mechanism, a series of mechanistic experiments were conducted. Mercury poisoning experiments were carried out to ascertain the homogeneous or heterogeneous nature of the catalytic system. The negligible

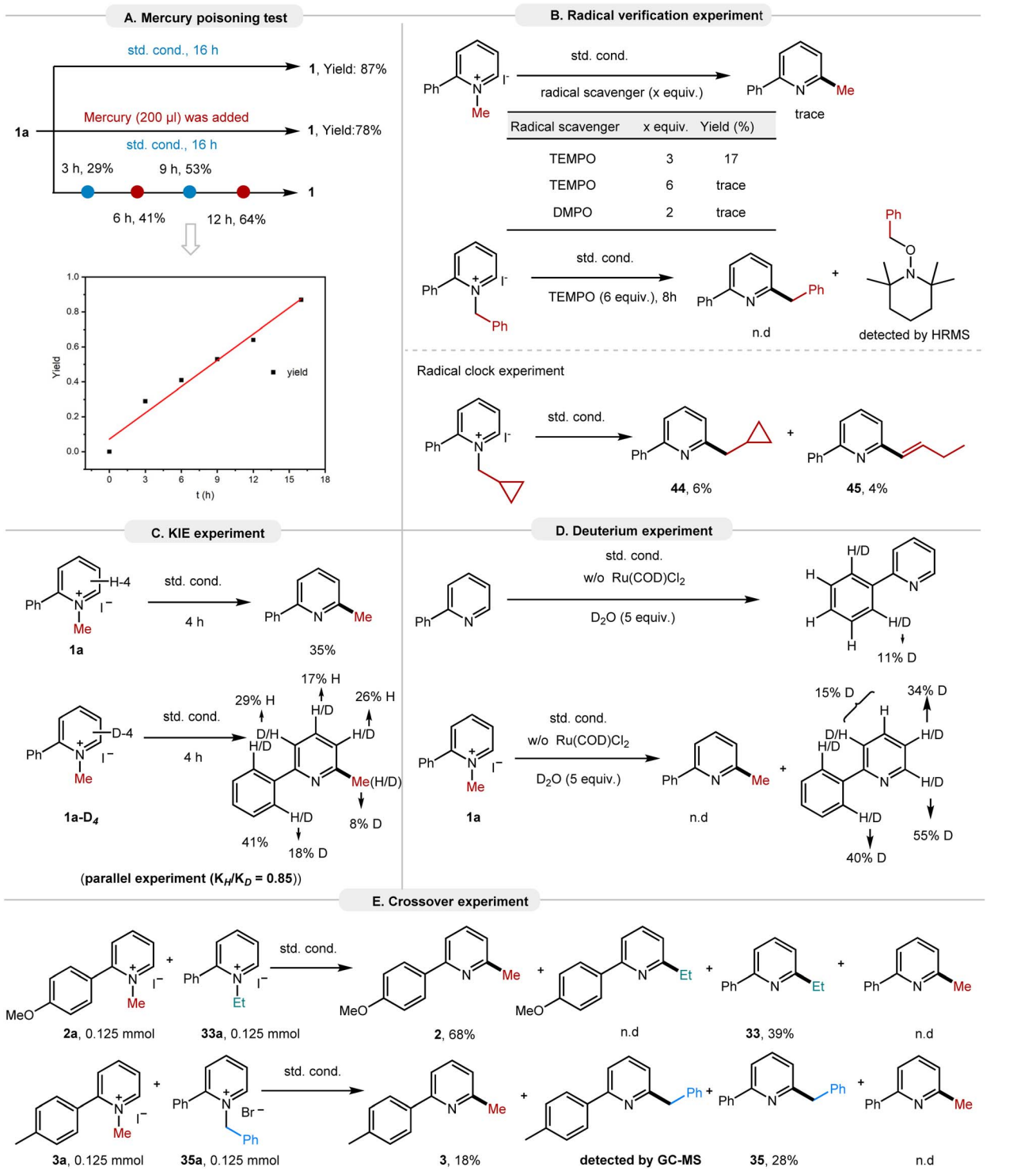


Scheme 4 Mechanistic study: (A) mercury poisoning test, (B) radical verification experiment, (C) KIE experiment, (D) deuterium experiment, and (E) crossover experiment.

change in reaction yield upon the addition of mercury, together with the observed near-linear correlation of yield over reaction time, indicated that the reaction proceeded *via* homogeneous catalysis (Scheme 4A). Subsequently, a series of control experiments were performed to elucidate whether the transformation follows a radical or ionic pathway (Scheme 4B). Under standard conditions, the addition of radical scavengers such as TEMPO or DMPO markedly suppressed the reaction yield. Notably, treatment of *N*-benzylpyridinium salts with TEMPO (6.0 equiv.) under standard conditions afforded the corresponding benzyl-TEMPO adducts, as confirmed by HRMS analysis. Furthermore, a radical clock experiment using *N*-cyclopropylmethylpyridinium iodide produced both the desired cyclopropylmethyl-migrated product **45** and a ring-opened derivative **46**. The formation of the latter serves as a diagnostic indicator of radical-induced cyclopropyl ring opening, providing direct evidence for the involvement of radical intermediates in this *N*-alkyl migration process.

Kinetic isotope effect (KIE) studies were subsequently conducted (Scheme 4C). No primary kinetic isotope effect (KIE) was observed from parallel reactions between **1a** and **1a-D$_4$**, suggesting that cleavage of the *ortho* C–H bond is not involved in the rate-determining step. It is noteworthy that deuterium from **1a-D$_4$** was found to be distributed among the *ortho* positions of the 2-phenyl group, the pyridine ring, and the 2-methyl group in the final product. In this context, a control experiment was performed, where **1a** was treated with stoichiometric CuI (without the Ru catalyst) and then quenched with $D_2O$. The target methyl-migration product **1** was not detected, whereas significant amounts of 2-phenylpyridine were formed. The recovered 2-phenylpyridine exhibited deuterium incorporation at both the pyridine ring and the *ortho* C–H bonds of the 2-phenyl group. Crucially, when 2-phenylpyridine itself was subjected to the same treatment, no analogous deuterium incorporation was observed (Scheme 4D). These results unambiguously indicate that *ortho* cupration is a key step in this transformation, a process that can occur with stoichiometric CuI, thereby supporting our proposed mechanistic pathway. Crossover experiments were conducted to distinguish between intra- and intermolecular *N*-alkyl migration pathways (Scheme 4E). Reactions of **2a** and **33a** afforded their respective products **2** (68%) and **33** (39%) exclusively, with no cross-migration products observed, indicating that the methyl and ethyl radicals are short-lived and solvent-caged. In contrast, a trace amount of the crossover product was detected by GC-MS in the **3a**/**35a** system, consistent with coupling between a 2-(*p*-methyl) pyridyl moiety and a benzyl radical. This observation indicates that the relatively stable benzyl radical can escape the solvent cage for intermolecular coupling, whereas less stable methyl and ethyl radicals cannot.

Based on the experimental evidence presented above, a plausible reaction mechanism is proposed in Scheme 5. The catalytically active Ru species **A** is generated *in situ via* metathesis between Ru(COD)Cl$_2$ and PivOK. Concurrently, substrate **1a** reacts with CuI with the aid of PivOK to generate the 2-pyridylidene–Cu(I) complex **B**.[20] The catalytic cycle is initiated by the transmetalation of **A** and **B** to form the pyridiniumyl-Ru(II)

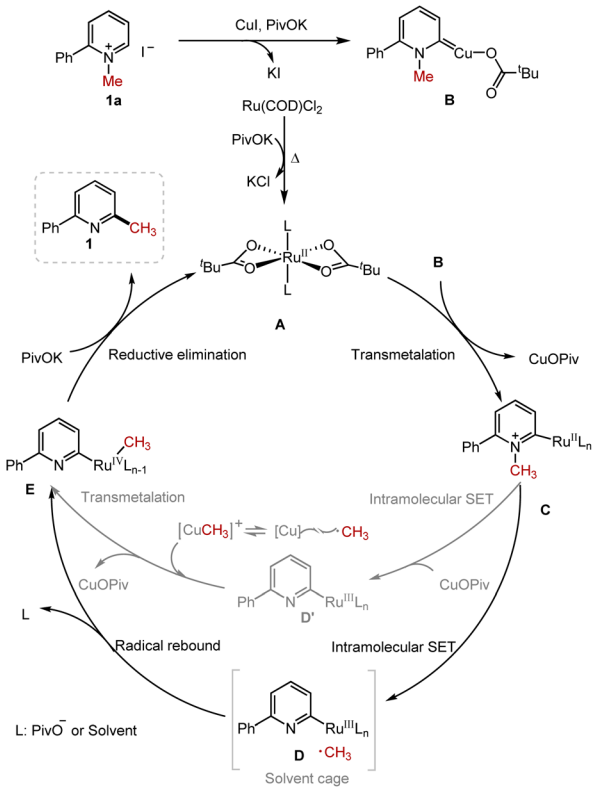


Scheme 5 Proposed mechanism.

intermediate **C**. Acting as an electron sink, the electron-deficient pyridiniumyl ligand drives an intramolecular single-electron transfer (SET) in **C**, resulting in homolytic cleavage of the $CH_3$–N bond. This cleavage produces the Ru(III) species **D** and releases a methyl radical. Within the solvent cage, radical recombination between **D** and the methyl radical forms Ru(IV) intermediate **E**. An alternative pathway involves the methyl radical escaping the solvent cage, stabilizing by binding to the copper centre,[22] and then being transferred to the ruthenium centre through transmetalation with Ru(III) complex **D′** to afford Ru(IV) intermediate **E**. Finally, reductive elimination from **E** delivers the migration product and regenerates the active Ru(II) catalyst **A**, closing the catalytic cycle. The involvement of Ru(III) and Ru(IV) species is further corroborated by X-ray photoelectron spectroscopy (XPS) analysis (SI Fig. S5).

## Conclusions

In conclusion, we have developed a synergistic Ru/Cu catalytic system that enables exclusive C2-selective methylation of pyridines. This strategy employs *N*-methylpyridinium salts as dual-function reagents, which concurrently serve as both the methyl source and the activated substrate, thereby accomplishing C2-methylation of pyridine with remarkable atom and step economy. Furthermore, the protocol was successfully extended to various *N*-alkylpyridinium salts, demonstrating broad applicability, and was effectively applied to the late-stage C2-methylation of pharmaceutical analogues containing pyridine motifs.

## Author contributions

S.-Y. H., and S. L. developed the methodology and performed the majority of the experiments. M.-Y. L., C. L. and S.-X. W. prepared some substrates. S.-Y. H., S. L., W.-C. X., J.-Q. X., X.-L. Z., R.-X. L., H. C. and H.-Y. F. prepared the manuscript. All authors have given approval to the final version of the manuscript.

## Conflicts of interest

There are no conflicts to declare.

## Data availability

The details of experimental procedures and the data about the findings of this study are available within the article and its supplementary information (SI). All data are available from the corresponding authors upon request. Source data are provided with this paper. Supplementary information: experimental details and characterization data for all products. See DOI: https://doi.org/10.1039/d5sc10082h.

## Acknowledgements

This work was supported by Sichuan Science and Technology Program (grant no. 2024YFFK0016) and Postgraduate Education and Teaching Reform Programme of Sichuan University (grant no. GSSCU2024058). We also thank Chunchun Zhang and Yunfei Tian from the Centre of Analysis & Testing, and Dongyan Deng and Jing Li from the College of Chemistry, Sichuan University for NMR, HRMS, XPS measurements.

## Notes and references

1 (*a*) R. W. Friesen, C. Brideau, C. C. Chan, S. Charleson, D. Deschanes, D. Visco, L. J. Xu and R. N. Young, *Med. Chem. Lett.*, 1998, **8**, 2777–2782; (*b*) E. J. Barreiro, A. E. Kümmerle and C. A. M. Fraga, *Chem. Rev.*, 2011, **111**, 5215–5246; (*c*) H. Schönherr and T. Cernak, *Angew. Chem., Int. Ed.*, 2013, **52**, 12256–12267; (*d*) D. A. DiRocco, K. Dykstra, S. Krska, P. Vachal, D. V. Conway and M. Tudge, *Angew. Chem., Int. Ed.*, 2014, **53**, 4802–4806; (*e*) J. Huang, Z. Chen and J. Wu, *ACS Catal.*, 2021, **11**, 10713–10732.

2 (*a*) E. Vitaku, D. T. Smith and J. T. Njardarson, *J. Med. Chem.*, 2014, **57**, 10257–10274; (*b*) C. M. Marshall, J. G. Federice, C. N. Bell, P. B. Cox and J. T. Njardarson, *J. Med. Chem.*, 2024, **67**, 11622–11655.

3 (*a*) J. Jin and D. W. C. MacMillan, *Nature*, 2015, **525**, 87–90; (*b*) W. Liu, X. Yang, Z. Z. Zhou and C. J. Li, *Chem*, 2017, **2**, 688–702; (*c*) T. McCallum, S. P. Pitre, M. Morin, J. C. Scaiano and L. Barriault, *Chem. Sci.*, 2017, **8**, 7412–7418; (*d*) S. Han, P. Chakrasali, J. Park, H. Oh, S. Kim, K. Kim, A. K. Pandey, S. H. Han, S. B. Han and I. S. Kim, *Angew. Chem., Int. Ed.*, 2018, **57**, 12737–12740; (*e*) T. J. Donohoe, A. Grozavu, H. B. Hepburn, E. P. Bailey and P. J. Lindsay-Scott, *Chem. Sci.*, 2020, **11**, 8595–8599.

4 F. O'Hara, D. G. Blackmond and P. S. Baran, *J. Am. Chem. Soc.*, 2013, **135**, 12122–12134.

5 H. Shi, P. Wang, S. Suzuki, M. E. Farmer and J. Q. Yu, *J. Am. Chem. Soc.*, 2016, **138**, 14876–14879.

6 Z. H. Chen, L. Liu, Y. B. Wang, H. Luo, Z. L. Tang, X. Y. Zhou and X. C. Wang, *J. Am. Chem. Soc.*, 2025, **147**, 36882–36889.

7 C. S. Giam and S. D. Abbott, *J. Am. Chem. Soc.*, 1971, **93**, 1294–1296.

8 For selected recent examples for alkylation of pyridine through Minisci reaction, see: (*a*) P. D. Bacoș, A. S. K. Lahdenperä and R. J. Phipps, *Acc. Chem. Res.*, 2023, **56**, 2037–2049; (*b*) Z. Liu, L. Peng and H. Huang, *Chem. Commun.*, 2025, **61**, 14490–14509; (*c*) M. Li, J. Yang, K. Qiao, F. Li and L. Shi, *Org. Lett.*, 2026, **28**, 831–836.

9 For selected recent examples for C2 or C4 selective methylation of pyridine, see: (*a*) F. Rammal, D. Gao, S. Boujnah, A. C. Gaumont, A. A. Hussein and S. Lakhdar, *Org. Lett.*, 2020, **22**, 7671–7675; (*b*) M. Kim, Y. Koo and S. Hong, *Acc. Chem. Res.*, 2022, **55**, 3043–3056; (*c*) M. Duan, Q. Shao, Q. Zhou, P. S. Baran and K. N. Houk, *Nat. Commun.*, 2024, **15**, 4630; (*d*) W. Jo, C. Thangsrikeattigun, C. Ryu, S. Han, C. Oh, M. H. Baik and S. H. Cho, *J. Am. Chem. Soc.*, 2025, 8597–8660.

10 (*a*) W. Jo, J. Kim, S. Choi and S. H. Cho, *Angew. Chem., Int. Ed.*, 2016, **55**, 9690–9694; (*b*) W. Jo, S. Y. Baek, C. Hwang, J. Heo, M. H. Baik and S. H. Cho, *J. Am. Chem. Soc.*, 2020, **142**, 13235–13245.

11 For selected examples for Minisci-type radical methylation, see: (*a*) R. S. J. Proctor and R. J. Phipps, *Angew. Chem., Int. Ed.*, 2019, **58**, 13666–13699; (*b*) J. H. Kim, T. Constantin, M. Simonetti, J. Llaveria, N. S. Sheikh and D. Leonori, *Nature*, 2021, **595**, 677–683; (*c*) L. Cao, H. Zhao, R. Guan, H. Jiang, P. H. Dixneuf and M. Zhang, *Nat. Commun.*, 2021, **12**, 4206; (*d*) H. Jia, Z. Tan and M. Zhang, *Acc. Chem. Res.*, 2024, **57**, 795–813.

12 For selected examples for *N*-functionalized pyridinium salts as versatile radical precursors, see: (*a*) F. S. He, S. Ye and J. Wu, *ACS Catal.*, 2019, **9**, 8943–8960; (*b*) S. L. Rössler, B. J. Jelier, E. Magnier, G. Dagousset, E. M. Carreira and A. Togni, *Angew. Chem., Int. Ed.*, 2020, **59**, 9264–9280; (*c*) Y. Wang, Y. Bao, M. Tang, Z. Ye, Z. Yuan and G. Zhu, *Chem. Commun.*, 2022, **58**, 3847–3864; (*d*) S. Singh, D. Gambhir and R. P. Singh, *Chem. Commun.*, 2025, **61**, 3436–3446.

13 A. C. Sun, E. J. McClain, J. W. Beatty and C. R. J. Stephenson, *Org. Lett.*, 2018, **20**, 3487–3490.

14 (*a*) I. Kim, B. Park, G. Kang, J. Kim, H. Jung, H. Lee, M. H. Baik and S. Hong, *Angew. Chem., Int. Ed.*, 2018, **57**, 15517–15522; (*b*) J. Jeon, Y. T. He, S. Shin and S. Hong, *Angew. Chem., Int. Ed.*, 2019, **59**, 281–285; (*c*) I. Kim, S. Park and S. Hong, *Org. Lett.*, 2020, **22**, 8730–8734; (*d*) B. Kweon, C. Kim, S. Kim and S. Hong, *Angew. Chem., Int. Ed.*, 2021, **60**, 26813–26821.

15 H. Liu, F. Wu, Z. Wan, C. Yue, C. Wang, C. Liu, Y. Li, Z. Fang, H. Qin and Z. Yang, *Org. Chem. Front.*, 2025, 5279–5284.

16 For selected examples for *N*-oxygen/nitrogen-substituted pyridinium salts as versatile alkyl radical precursors, see: (*a*) J. R. Chen, X. Q. Hu, L. Q. Lu and W. J. Xiao, *Chem. Soc. Rev.*, 2016, **45**, 2044–2056; (*b*) W. S. Ham, J. Hillenbrand, J. Jacq, C. Genicot and T. Ritter, *Angew. Chem., Int. Ed.*, 2019, **58**, 532–536; (*c*) I. Kim, G. Kang, K. Lee, B. Park, D. Kang, H. Jung, Y. T. He, M. H. Baik and S. Hong, *J. Am. Chem. Soc.*, 2019, **141**, 9239–9248.

17 For selected examples for Katritzky salts as versatile alkyl radical precursors, see: (*a*) J. J. Wu, P. S. Grant, X. B. Li, A. Noble and V. K. Aggarwal, *Angew. Chem., Int. Ed.*, 2019, **58**, 5697–5701; (*b*) S. Z. Sun, Y. M. Cai, D. L. Zhang, J. B. Wang, H. Q. Yao, X. Y. Rui, R. Martin and M. Shang, *J. Am. Chem. Soc.*, 2022, **144**, 1130–1137.

18 For selected examples for *N*-functionalized pyridinium salts as versatile alkyl radical precursors, see: (*a*) F. J. R. Klauck, M. J. James and F. Glorius, *Angew. Chem., Int. Ed.*, 2017, **56**, 12336–12339; (*b*) Y. Wei, Q. Wang and M. J. Koh, *Angew. Chem., Int. Ed.*, 2022, **62**, e202214247; (*c*) C. Wang, P. Dam, M. Elghobashy, A. Brückner, J. Rabeah, L. M. Azofra and O. El-Sepelgy, *ACS Catal.*, 2023, **13**, 14205–14212; (*d*) C. Chen, X. Shen, S. Guo, R. Yan, H. Yu, Y. Han, Q. Sun and S. Zhu, *Chem. Commun.*, 2025, 8556–8559; (*e*) L. Salamone, X. Vanderbiest and O. Riant, *Org. Lett.*, 2025, **27**, 2569–2575.

19 (*a*) C. S. Sevov, D. P. Hickey, M. E. Cook, S. G. Robinson, S. Barnett, S. D. Minteer, M. S. Sigman and M. S. Sanford, *J. Am. Chem. Soc.*, 2017, **139**, 2924–2927; (*b*) Z. Qiu and C. N. Neumann, *ACS Org. Inorg. Au*, 2023, **4**, 1–25.

20 (*a*) M. Roselló-Merino, J. Díez and S. Conejero, *Chem. Commun.*, 2010, **46**, 9247–9249; (*b*) B. Song, T. Knauber and L. J. Gooßen, *Angew. Chem., Int. Ed.*, 2013, **52**, 2954–2958; (*c*) C. Yin, K. Zhong, W. Li, X. Yang, R. Sun, C. Zhang, X. L. Zheng, M. L. Yuan, R. X. Li, Y. Lan, H. Y. Fu and H. Chen, *Adv. Synth. Catal.*, 2018, **360**, 3990–3998; (*d*) Y. Huang and M. K. Brown, *Angew. Chem.*, 2019, **131**, 6109–6113; (*e*) J. Tang, S. Li, J. Zhang, M. X. Yan, Y. L. Shi, X. L. Zheng, M. L. Yuan, H. Y. Fu, R. X. Li and H. Chen, *Org. Lett.*, 2023, **25**, 5203–5208.

21 For selected examples for MLCT, see: (*a*) A. Cadranel, P. S. Oviedo, G. E. Pieslinger, S. Yamazaki, V. D. Kleiman, L. M. Baraldo and D. M. Guldi, *Chem. Sci.*, 2017, **8**, 7434–7442; (*b*) A. N. Micci, J. E. Fumo, R. D. Pike and D. Lionetti, *Organometallics*, 2024, **43**, 1912–1921; (*c*) Y. Wang, B. Yuan, X. Chang and L. Ackermann, *Chem*, 2025, **11**, 102387; (*d*) J. H. Docherty, M. D. Hareram, L. M. Nichols, I. Pérez-Ortega, I. J. Vitorica-Yrezabal and I. Larrosa, *Nat. Catal.*, 2025, **8**, 301–314.

22 G. Ferraudi, *Chem. Inform.*, 1978, **9**, 139.